Available online at www.sciencedirect.com
SCIENCE DIRECT®
Computers and Structures 81 (2003) 2467–2478
Computers & Structures
www.elsevier.com/locate/compstruc

Dynamic analysis of high speed railway bridge under articulated trains

He Xia [a], Nan Zhang [a], Guido De Roeck [b,*]

[a] School of Civil Engineering and Architecture, Northern Jiaotong University, Beijing 100044, China
[b] Department of Civil Engineering, Catholic University of Leuven, Kasteelpark Arenberg 40, B-3001 Heverlee, Belgium

Received 23 July 2002; accepted 3 July 2003

Abstract

The problem of vehicle–bridge dynamic interaction system under articulated high speed trains is studied in this paper. A dynamic interaction model of the bridge-articulated train system is established, which is composed of an articulated vehicle element model and a finite element bridge model. The vehicle model is established according to the structure and suspending properties of the articulated vehicles. A computer simulation program is worked out. As an example, the case of the Thalys articulated train passing along the Antoing Bridge on the Paris–Brussels high speed railway line is analyzed. The dynamic responses of the bridge and the vehicles are calculated. The proposed analysis model and the solution method are verified through the comparison between the calculated results and the in situ measured data. The vibration behaviour of the articulated trains is discussed.

Keywords: Articulated trains; Vehicle–bridge system; Dynamic interaction; Experiment

1. Introduction

Driven by a fast developing economy and supported by technologic evolutions, the modernization of railway network is progressing. From the 1960s, the maximum record of the train speed has been increased continuously. The experimental maximum speed of the TGV train in France has reached 515 km/h. At the same time, the safety and the comfort of passenger trains should still be kept at the same high level. The linking and suspension systems of train vehicles are different in diverse types of high-speed trains. In Japan, each vehicle of the E2 train has a separated traction system. The ICE train in Germany adopts a traditional connection between the vehicles and the traction power is provided by locomotives. Although the TGV train is composed of locomotive and passenger cars, a unique link pattern is used between passenger cars so that the whole train is articulated. Adjacent cars are sharing the same bogie and are linked by an elastic hinge. The articulated train has distinct dynamic characteristics and therefore, its study is of great significance to the running stability of the vehicles. An important study object is the dynamic interaction between vehicles and bridges under the passage of high speed articulated trains.

The dynamic response of railway bridges under train loads is one of the fundamental problems to be solved in railway bridge design and maintenance. Therefore, great efforts have been continuously spent to the subject of dynamic interaction of vehicles and bridges. The research work on this subject has a long history of more than one hundred years. Especially in the last decades, increasingly sophisticated analytical models have been successfully developed by researchers in China and abroad [2–5,7,9–14]. Based on these models, vertical and

* Corresponding author. Tel.: +32-16321666; fax: +32-1321988.
E-mail address: guido.deroeck@bwk.kuleuven.ac.be (G. De Roeck).

0045-7949/$ - see front matter © 2003 Elsevier Ltd. All rights reserved.
doi:10.1016/S0045-7949(03)00309-2

lateral dynamic interactions of the train–bridge system have been studied and many useful results applied to practical bridge engineering. There have also been some papers published on the dynamic behaviors of articulated trains [6,8,15,16].

The European Rail Research Institute (ERRI) has co-ordinated and performed railway research programmes e.g. on interaction between vehicles and track, determination of dynamic forces in bridges, braking and acceleration forces on bridges and interaction between track and structures [17]. None of the published reports treats the interaction problem as presented in this paper, i.e. in case of articulated trains.

In this paper, the case of the Thalys train passing through a double-track, U-shaped, 50 m long PC girder on the Paris–Brussels high speed railway line is studied. The dynamic responses of the bridge and the articulated vehicles are calculated and experimentally measured. Based on these results the dynamic behaviour of the articulated train is commented.

2. Analysis method of bridge–vehicle interaction system

2.1. Vehicle model

A single Thalys high speed train is composed of one locomotive followed by one transition carriage, six normal articulated cars, one transition carriage and one locomotive. The composition of the first half of a single Thalys train is shown in Fig. 1. The front and the rear locomotives have each two independent bogies, and can be modeled by the traditional method into three rigid bodies, each comprising 15DOFs [11–13]. The transition carriage has an independent bogie at the locomotive end and shares an articulated bogie with the adjacent passenger car. The normal passenger cars share both bogies with the adjacent cars or the transition carriage. There are in total 10 vehicles, 13 bogies and 26 wheel-sets in a Thalys train. Since the 2nd to the 9th vehicles are articulated with each other, they are treated as a group. The whole group of these eight vehicles with nine bogies can be modeled as 17 rigid bodies and 85DOFs in total. With the 30DOFs of the two locomotives, the total number of the DOFs of the whole train model is 115.

In modeling, the whole articulated train group is regarded as a series of articulated vehicle elements composed of car bodies, bogies and wheel sets, as is shown in Fig. 2. In each articulated vehicle element, the car body is connected to the front bogie with transverse and vertical springs and dampers, and to the following car body with the central elastic hinge. The central hinge between the two car bodies is also modeled by transverse springs and dampers. In this way, the car body in an articulated vehicle element is connected through three elastic or damping points to the adjacent rigid bodies, forming a geometrically stable system. The four dampers between the two adjacent car bodies also play the role of reducing the nodding and the yawing movements of the

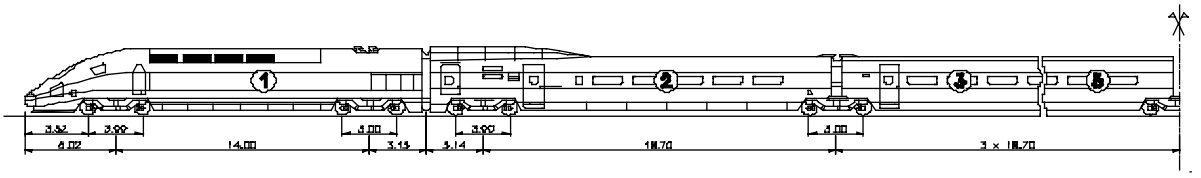

Fig. 1. High speed Thalys train composition.

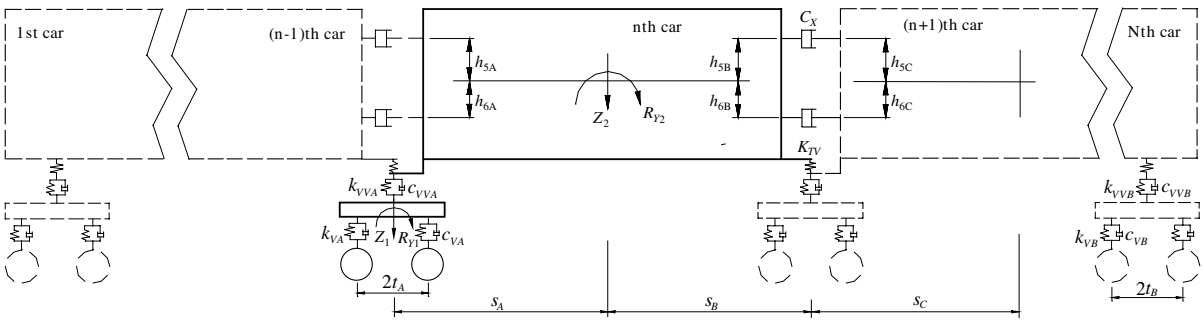

Fig. 2. Dynamic model of articulated vehicles.

car bodies, which are modeled as viscous damping in the model. This treatment has a particular advantage that all the three types of vehicles: the 1st transition carriage with front independent bogie rear articulated bogie, the normal cars with two articulated bogies, and the last transition carriage with front articulated bogie rear independent bogie, can be modeled by identical vehicle elements, with only a few components changed, as is shown in the following descriptions, which is also very convenient for programming.

There are two suspension systems in an articulated vehicle. In the primary suspension, the wheels are elastically connected to the bogie frame, laterally by the positioning rubber blocks in lateral and vertically by the axle-box springs and dampers. The primary suspension system can thus be simplified as an elastic system, with the bogies and wheel-sets linked by the lateral and vertical springs and dampers.

In the secondary suspension, between the car body and the bogies, flexible air springs are mounted which have little vertical damping. The secondary suspension system is also regarded as elastic, but its lateral springs and dampers are between the car body and the bogies.

Each car body and bogie in the articulated vehicle element, has five degrees of freedom, which are the transverse Y, rolling R_X, yawing R_Z, floating Z and nodding R_Y movements.

It can be noticed that there are only transverse and vertical springs but no dampers at the central hinges, and only four longitudinal dampers but no springs between the car bodies. To keep the consistency in the expressions of stiffness and damping matrices of the articulated vehicle element, both springs and dampers are set at the central hinges between the car bodies. The nominal spring coefficients or damping factors will be put equal to zero in the calculation. In this way, the damping matrix and the force vector can be directly obtained by substituting the damping coefficient "c" into the spring coefficient "k" of the stiffness matrix in the following derivations.

The total mass, stiffness and damping matrices of the articulated vehicle group can be established by assembling the corresponding element matrices together. The motion equations of the articulated vehicle group can be expressed as:

$$[M]\{\ddot{v}\} + [C]\{\dot{v}\} + [K]\{v\} = \{F\} \tag{1}$$

In Eq. (1), $\{v\}$ is the displacement vector of the articulated vehicle group:

$$\{v\} = [v_{b1}, v_{v1}, v_{b2}, v_{v2}, \ldots, v_{bn}, v_{vn}, \ldots, v_{bN}, v_{vN}, v_{bN+1}]^{\mathrm{T}} \tag{2}$$

where $\{v_{bn}\} = [Y_{bn}, R_{Xbn}, R_{Zbn}, Z_{bn}, R_{Ybn}]^{\mathrm{T}}$ and $\{v_{vn}\} = [Y_{vn}, R_{Xvn}, R_{Zvn}, Z_{vn}, R_{Yvn}]^{\mathrm{T}}$ are the sub-vectors of the nth bogie and the nth car body of the nth articulated vehicle element, including their lateral, rolling, yawing, floating and nodding movements, respectively; N is the number of the articulated vehicles and $N+1$ is therefore the number of the bogies of the articulated train group including the two transition carriages.

$[M]$ is the mass matrix of the articulated vehicle group:

$$[M] = \mathrm{diag}[M_{b1}, M_{v1}, M_{b2}, M_{v2}, \ldots, M_{bn}, M_{vn}, \ldots, M_{bN}, M_{vN}, M_{bN+1}] \tag{3}$$

where $[M_{bn}] = \mathrm{diag}[M_{Ybn}, J_{Xbn}, J_{Zbn}, M_{Zbn}, J_{Ybn}]$ and $[M_{vn}] = \mathrm{diag}[M_{Yvn}, J_{Xvn}, J_{Zvn}, M_{Zvn}, J_{Yvn}]$ are the lumped mass submatrices of the nth bogie and the nth vehicle body of the nth articulated vehicle element, with M denoting the rigid mass for lateral and floating movements, J the mass moment for rolling, yawing and nodding movements, respectively.

In the next matrices, k_{VA}, k_{VB}, k_{HA} and k_{HB} are the primary suspension spring coefficients at each side of the bogies, with the subscripts V and H denoting vertical and horizontal, A and B denoting the front and the rear bogie (B only for the transition carriages with two bogies), respectively. k_{VVA}, k_{VVB}, k_{HHA} and k_{HHB} are the secondary suspension spring coefficients at each side of the bogie. k_{TH}, k_{TV}, k_{THD} and k_{TVD} are the spring coefficients at the central elastic hinge in the back and the front of this vehicle. k_X and $k_{X\mathrm{D}}$ are the longitudinal spring coefficients between the two car bodies in the back and the front of this car body. t_{A} and t_{B} (B only for the transition carriages with two bogies) are the half axle intervals of the bogies. s_{A} and s_{B} are the distances between the current car body center and the bogie centers. s_{C} is the distance between the following car body center and its front bogie center. $b_{1\mathrm{A}}$, $b_{1\mathrm{B}}$, $b_{2\mathrm{A}}$ and $b_{2\mathrm{B}}$ are the half lateral span of the primary and secondary springs. b_3 is the half transverse span of the longitudinal spring between the car bodies. $h_{1\mathrm{A}}$, $h_{1\mathrm{B}}$ and $h_{1\mathrm{C}}$ are the vertical distances between the car body center and the secondary suspensions at the position of the front of this car body, the back of this car body and the front of the following car body. $h_{2\mathrm{A}}$ and $h_{2\mathrm{B}}$ are the vertical distances between the bogie centers and the secondary suspensions. $h_{3\mathrm{A}}$ and $h_{3\mathrm{B}}$ are the vertical distances between the bogie centers and the axle centers. $h_{5\mathrm{A}}$, $h_{5\mathrm{B}}$ and $h_{5\mathrm{C}}$ are respectively the vertical distance between the current car body center and its front upper longitudinal springs at the position of the front of this car body, the back of this car body and the front of the following car body. $h_{6\mathrm{A}}$, $h_{6\mathrm{B}}$, $h_{6\mathrm{C}}$ are respectively the vertical distance between the current car body center and its front lower longitudinal springs at the position of the front of this car body, the back of this car body and the front of the following car body. Most of these parameters illustrated in Figs. 2 and 3.

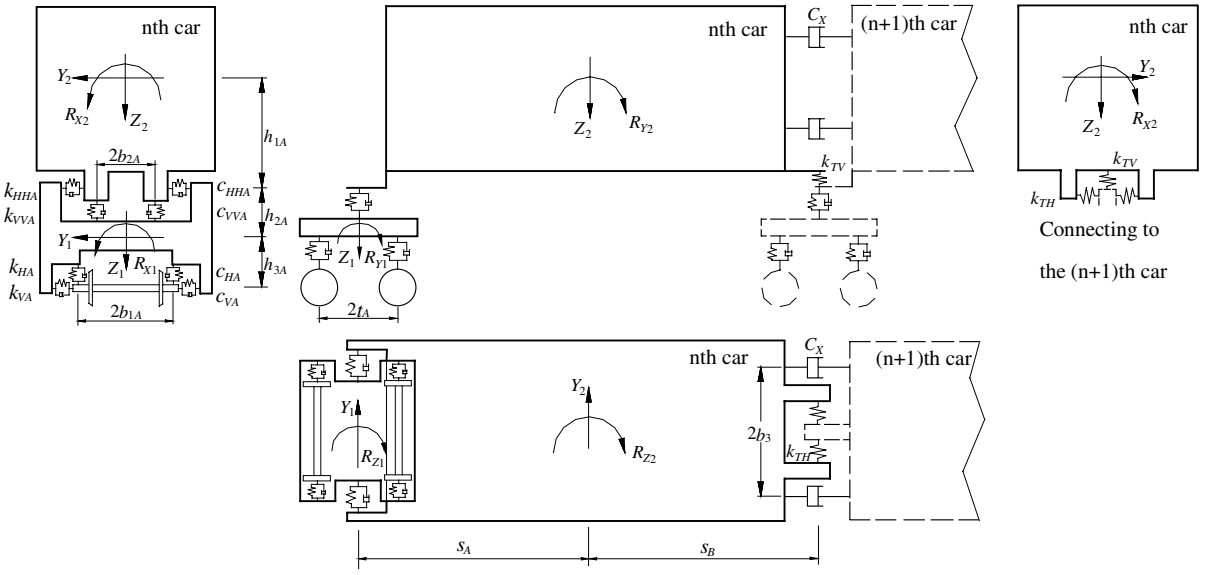

Fig. 3. Dynamic model of articulated vehicle element.

Since the vehicles of the group are only adjacently coupled with each other, the stiffness matrix $[K]$ is a tri-diagonal one:

$$[K]=\begin{bmatrix} K_{1,1} & K_{1,2} & \cdots & 0 & 0 & 0 & \cdots & 0 & 0 \\ K_{2,1} & K_{2,2} & \cdots & 0 & 0 & 0 & \cdots & 0 & 0 \\ \vdots & \vdots & \ddots & \vdots & \vdots & \vdots & \cdots & \vdots & \vdots \\ 0 & 0 & \cdots & K_{n-1,n-1} & K_{n-1,n} & 0 & \cdots & 0 & 0 \\ 0 & 0 & \cdots & K_{n,n-1} & K_{n,n} & K_{n,n+1} & \cdots & 0 & 0 \\ 0 & 0 & \cdots & & K_{n+1,n} & K_{n+1,n+1} & \cdots & 0 & 0 \\ \vdots & \vdots & \cdots & \vdots & \vdots & \vdots & \ddots & \vdots & \vdots \\ 0 & 0 & \cdots & 0 & 0 & 0 & \cdots & K_{N,N} & K_{N,N+1} \\ 0 & 0 & \cdots & 0 & 0 & 0 & \cdots & K_{N+1,N} & K_{N+1,N+1} \end{bmatrix} \tag{4}$$

In the matrix, $K_{n,n}$ is the 10×10 order stiffness matrix of the nth articulated vehicle element ($n=1,N$):

$$[K_{n,n}]=\begin{bmatrix} K^{b}_{n,n} & K^{bv}_{n,n} \\ K^{vb}_{n,n} & K^{v}_{n,n} \end{bmatrix}=\begin{bmatrix} K_{n1} & & & sym \\ 0 & K_{n2} & & \\ K_{n3} & 0 & K_{n4} & \\ 0 & K_{n5} & 0 & K_{n6} \end{bmatrix} \tag{5}$$

where K_{n1} and K_{n2} are the sub-stiffness matrices of the nth bogie:

$$[K_{n1}]=\begin{bmatrix} 4k_{\mathrm{HA}}+2k_{\mathrm{HHA}} & -4k_{\mathrm{HA}}h_{3\mathrm{A}}+2k_{\mathrm{HHA}}h_{2\mathrm{A}} & 0 \\ -4k_{\mathrm{HA}}h_{3\mathrm{A}}+2k_{\mathrm{HHA}}h_{2\mathrm{A}} & 4k_{\mathrm{HA}}h_{3\mathrm{A}}^2+4k_{\mathrm{VA}}b_{1\mathrm{A}}^2+2k_{\mathrm{HHA}}h_{2\mathrm{A}}^2+2k_{\mathrm{VVA}}b_{2\mathrm{A}}^2 & 0 \\ 0 & 0 & 4k_{\mathrm{HA}}t_{\mathrm{A}}^2 \end{bmatrix}$$

$$[K_{n2}]=\begin{bmatrix} 4k_{\mathrm{VA}}+2k_{\mathrm{VVA}} & 0 \\ 0 & 4k_{\mathrm{VA}}t_{\mathrm{A}}^2 \end{bmatrix}$$

K_{n3} and K_{n5} are the sub-stiffness matrices coupling the nth bogie and the nth vehicle body:

$$[K_{n3}]=\begin{bmatrix} -2k_{\mathrm{HHA}} & -2k_{\mathrm{HHA}}h_{2\mathrm{A}} & 0 \\ 2k_{\mathrm{HHA}}h_{1\mathrm{A}} & 2k_{\mathrm{HHA}}h_{1\mathrm{A}}h_{2\mathrm{A}}-2k_{\mathrm{VVA}}b_{2\mathrm{A}}^2 & 0 \\ -2k_{\mathrm{HHA}}s_{\mathrm{A}} & -2k_{\mathrm{HHA}}s_{\mathrm{A}}h_{2\mathrm{A}} & 0 \end{bmatrix}$$

$$[K_{n5}]=\begin{bmatrix} -2k_{\mathrm{VVA}} & 0 \\ 2k_{\mathrm{VVA}}s_{\mathrm{A}} & 0 \end{bmatrix}$$

K_{n4} and K_{n6} are the sub-stiffness matrices of the nth vehicle body. For the first transition carriage ($n=1$):

$$[K_{n4}]=\begin{bmatrix} 2k_{\mathrm{HHA}} & & \mathrm{Sym} \\ -2k_{\mathrm{HHA}}h_{1\mathrm{A}} & 2k_{\mathrm{HHA}}h_{1\mathrm{A}}^2+2k_{\mathrm{VVA}}b_{2\mathrm{A}}^2 & \\ 2k_{\mathrm{HHA}}s_{\mathrm{A}} & -2k_{\mathrm{HHA}}s_{\mathrm{A}}h_{1\mathrm{A}} & 2k_{\mathrm{HHA}}s_{\mathrm{A}}^2 \end{bmatrix} + \begin{bmatrix} k_{\mathrm{TH}} & & \mathrm{Sym} \\ -k_{\mathrm{TH}}h_{1\mathrm{B}} & k_{\mathrm{TH}}h_{1\mathrm{B}}^2 & \\ k_{\mathrm{TH}}s_{\mathrm{B}} & -k_{\mathrm{TH}}s_{\mathrm{B}}h_{1\mathrm{B}} & k_{\mathrm{TH}}s_{\mathrm{B}}^2+4k_X b_{3\mathrm{B}}^2 \end{bmatrix}$$

$$[K_{n7}]=\begin{bmatrix} 4k_{\mathrm{HB}}+2k_{\mathrm{HHB}} & -4k_{\mathrm{HB}}h_{3\mathrm{B}}+2k_{\mathrm{HHB}}h_{2\mathrm{B}} & 0 \\ -4k_{\mathrm{HB}}h_{3\mathrm{B}}+2k_{\mathrm{HHB}}h_{2\mathrm{B}} & 4k_{\mathrm{HB}}h_{3\mathrm{B}}^2+4k_{\mathrm{VB}}b_{1\mathrm{B}}^2+2k_{\mathrm{HHB}}h_{2\mathrm{B}}^2+2k_{\mathrm{VVB}}b_{2\mathrm{B}}^2 & 0 \\ 0 & 0 & 4k_{\mathrm{HB}}t_{\mathrm{B}}^2 \end{bmatrix}$$

$$[K_{n6}]=\begin{bmatrix} 2k_{\mathrm{VVA}} & -2k_{\mathrm{VVA}}s_{\mathrm{A}} \\ -2k_{\mathrm{VVA}}s_{\mathrm{A}} & 2k_{\mathrm{VVA}}s_{\mathrm{A}}^2 \end{bmatrix} + \begin{bmatrix} k_{\mathrm{TV}} & -k_{\mathrm{TV}}s_{\mathrm{B}} \\ -k_{\mathrm{TV}}s_{\mathrm{B}} & k_{\mathrm{TV}}s_{\mathrm{B}}^2+2k_X h_{5\mathrm{B}}^2+2k_X h_{6\mathrm{B}}^2 \end{bmatrix}$$

For the intermediate articulated cars ($1 < n < N$):

$$[K_{n4}]=\begin{bmatrix} k_{\mathrm{THD}} & & \mathrm{Sym} \\ -k_{\mathrm{THD}}h_{1\mathrm{A}} & k_{\mathrm{THD}}h_{1\mathrm{A}}^2 & \\ k_{\mathrm{THD}}s_{\mathrm{A}} & -k_{\mathrm{THD}}s_{\mathrm{A}}h_{1\mathrm{A}} & k_{\mathrm{THD}}s_{\mathrm{A}}^2+4k_{X\mathrm{D}}b_{3\mathrm{A}}^2 \end{bmatrix} + \begin{bmatrix} 2k_{\mathrm{HHA}} & & \mathrm{Sym} \\ -2k_{\mathrm{HHA}}h_{1\mathrm{A}} & 2k_{\mathrm{HHA}}h_{1\mathrm{A}}^2+2k_{\mathrm{VVA}}b_{2\mathrm{A}}^2 & \\ 2k_{\mathrm{HHA}}s_{\mathrm{A}} & -2k_{\mathrm{HHA}}s_{\mathrm{A}}h_{1\mathrm{A}} & 2k_{\mathrm{HHA}}s_{\mathrm{A}}^2 \end{bmatrix} + \begin{bmatrix} k_{\mathrm{TH}} & & \mathrm{Sym} \\ -k_{\mathrm{TH}}h_{1\mathrm{B}} & k_{\mathrm{TH}}h_{1\mathrm{B}}^2 & \\ -k_{\mathrm{TH}}s_{\mathrm{B}} & k_{\mathrm{TH}}s_{\mathrm{B}}h_{1\mathrm{B}} & k_{\mathrm{TH}}s_{\mathrm{B}}^2+4k_X b_{3\mathrm{B}}^2 \end{bmatrix}$$

$$[K_{n6}]=\begin{bmatrix} k_{\mathrm{TVD}} & -k_{\mathrm{TVD}}s_{\mathrm{A}} \\ -k_{\mathrm{TVD}}s_{\mathrm{A}} & k_{\mathrm{TVD}}s_{\mathrm{A}}^2+2k_{X\mathrm{D}}h_{5\mathrm{A}}^2+2k_{X\mathrm{D}}h_{6\mathrm{A}}^2 \end{bmatrix} + \begin{bmatrix} 2k_{\mathrm{VVA}} & -2k_{\mathrm{VVA}}s_{\mathrm{A}} \\ -2k_{\mathrm{VVA}}s_{\mathrm{A}} & 2k_{\mathrm{VVA}}s_{\mathrm{A}}^2 \end{bmatrix} + \begin{bmatrix} k_{\mathrm{TV}} & k_{\mathrm{TV}}s_{\mathrm{B}} \\ k_{\mathrm{TV}}s_{\mathrm{B}} & k_{\mathrm{TV}}s_{\mathrm{B}}^2+2k_X h_{5\mathrm{B}}^2+2k_X h_{6\mathrm{B}}^2 \end{bmatrix}$$

For the last transition carriage ($n = N$):

$$[K_{n4}]=\begin{bmatrix} k_{\mathrm{THD}} & & \mathrm{Sym} \\ -k_{\mathrm{THD}}h_{1\mathrm{A}} & k_{\mathrm{THD}}h_{1\mathrm{A}}^2 & \\ k_{\mathrm{THD}}s_{\mathrm{A}} & -k_{\mathrm{THD}}s_{\mathrm{A}}h_{1\mathrm{A}} & k_{\mathrm{THD}}s_{\mathrm{A}}^2+4k_{X\mathrm{D}}b_{3\mathrm{A}}^2 \end{bmatrix} + \begin{bmatrix} 2k_{\mathrm{HHA}} & & \mathrm{Sym} \\ -2k_{\mathrm{HHA}}h_{1\mathrm{A}} & 2k_{\mathrm{HHA}}h_{1\mathrm{A}}^2+2k_{\mathrm{VVA}}b_{2\mathrm{A}}^2 & \\ 2k_{\mathrm{HHA}}s_{\mathrm{A}} & -2k_{\mathrm{HHA}}s_{\mathrm{A}}h_{1\mathrm{A}} & 2k_{\mathrm{HHA}}s_{\mathrm{A}}^2 \end{bmatrix} + \begin{bmatrix} 2k_{\mathrm{HHB}} & & \mathrm{Sym} \\ -2k_{\mathrm{HHB}}h_{1\mathrm{B}} & 2k_{\mathrm{HHB}}h_{1\mathrm{B}}^2+2k_{\mathrm{VVB}}b_{2\mathrm{B}}^2 & \\ -2k_{\mathrm{HHB}}s_{\mathrm{B}} & 2k_{\mathrm{HHB}}s_{\mathrm{B}}h_{1\mathrm{B}} & 2k_{\mathrm{HHB}}s_{\mathrm{B}}^2 \end{bmatrix}$$

$$[K_{n6}]=\begin{bmatrix} k_{\mathrm{TVD}} & -k_{\mathrm{TVD}}s_{\mathrm{A}} \\ -k_{\mathrm{TVD}}s_{\mathrm{A}} & k_{\mathrm{TVD}}s_{\mathrm{A}}^2+2k_{X\mathrm{D}}h_{5\mathrm{A}}^2+2k_{X\mathrm{D}}h_{6\mathrm{A}}^2 \end{bmatrix} + \begin{bmatrix} 2k_{\mathrm{VVA}} & -2k_{\mathrm{VVA}}s_{\mathrm{A}} \\ -2k_{\mathrm{VVA}}s_{\mathrm{A}} & 2k_{\mathrm{VVA}}s_{\mathrm{A}}^2 \end{bmatrix} + \begin{bmatrix} 2k_{\mathrm{VVB}} & 2k_{\mathrm{VVB}}s_{\mathrm{B}} \\ 2k_{\mathrm{VVB}}s_{\mathrm{B}} & 2k_{\mathrm{VVB}}s_{\mathrm{B}}^2 \end{bmatrix}$$

$K_{N+1,N+1}$ in Eq. (4) is the 5×5 order stiffness matrix of the last $(N+1)$th independent bogie:

$$[K_{N+1,N+1}]=\begin{bmatrix} K_{n7} & 0 \\ 0 & K_{n8} \end{bmatrix} \tag{6}$$

where:

$$[K_{n8}]=\begin{bmatrix} 4k_{\mathrm{VB}}+2k_{\mathrm{VVB}} & 0 \\ 0 & 4k_{\mathrm{VB}}t_{\mathrm{B}}^2 \end{bmatrix}$$

For $n < N$, $K_{n+1,n}$ and $K_{n,n+1}^{\mathrm{T}}$ in Eq. (4) are the 10×10 stiffness matrices coupling the nth vehicle element and the following rigid body:

$$[K_{n+1,n}]=[K_{n,n+1}^{\mathrm{T}}]=\begin{bmatrix} 0 & 0 & 0 & 0 \\ 0 & 0 & 0 & 0 \\ 0 & 0 & K_{n9} & 0 \\ 0 & 0 & 0 & K_{n10} \end{bmatrix} \tag{7}$$

where K_{n9} and K_{n10} are the sub-stiffness matrices coupling the nth and the $n+1$th vehicle bodies:

$$[K_{n9}]=\begin{bmatrix} -k_{\mathrm{TH}} & k_{\mathrm{TH}}h_{1\mathrm{B}} & k_{\mathrm{TH}}s_{\mathrm{B}} \\ k_{\mathrm{TH}}h_{1\mathrm{C}} & -k_{\mathrm{TH}}h_{1\mathrm{B}}h_{1\mathrm{C}} & -k_{\mathrm{TH}}h_{1\mathrm{C}}s_{\mathrm{B}} \\ -k_{\mathrm{TH}}s_{\mathrm{C}} & k_{\mathrm{TH}}s_{\mathrm{C}}h_{1\mathrm{B}} & k_{\mathrm{TH}}s_{\mathrm{B}}s_{\mathrm{C}}+4k_X b_{3\mathrm{B}}b_{3\mathrm{C}} \end{bmatrix}$$

$$[K_{n10}]=\begin{bmatrix} -k_{\mathrm{TV}} & -k_{\mathrm{TV}}s_{\mathrm{B}} \\ k_{\mathrm{TV}}s_{\mathrm{C}} & k_{\mathrm{TV}}s_{\mathrm{B}}s_{\mathrm{C}}+2k_X(h_{5\mathrm{B}}h_{5\mathrm{C}}+h_{6\mathrm{B}}h_{6\mathrm{C}}) \end{bmatrix}$$

When $n = N$, $K_{N+1,N}$ and $K_{N,N+1}^{\mathrm{T}}$ in Eq. (4) become the 5×10 stiffness matrices coupling the last (Nth) vehicle body and the last $(N+1)$th bogie:

$$[K_{N+1,N}]=[K_{N,N+1}]^{\mathrm{T}}=\begin{bmatrix} 0 & 0 & K_{N11} & 0 \\ 0 & 0 & 0 & K_{N12} \end{bmatrix} \tag{8}$$

where:

$$[K_{11}]=\begin{bmatrix} -2k_{\mathrm{HHB}} & 2k_{\mathrm{HHB}}h_{1\mathrm{B}} & 2k_{\mathrm{HHB}}s_{\mathrm{B}} \\ -2k_{\mathrm{HHB}}h_{2\mathrm{B}} & 2k_{\mathrm{HHB}}h_{1\mathrm{B}}h_{2\mathrm{B}}-2k_{\mathrm{VVB}}b_{2\mathrm{B}}^2 & 2k_{\mathrm{HHB}}s_{\mathrm{B}}h_{2\mathrm{B}} \\ 0 & 0 & 0 \end{bmatrix}$$

$$[K_{12}]=\begin{bmatrix} -2k_{\mathrm{HHB}} & -2k_{\mathrm{VVB}}s_{\mathrm{B}} \\ 0 & 0 \end{bmatrix}$$

In Eq. (1), $\{F\}$ is the force vector of the articulated vehicle group:

$$\{F\}=[F_{b1},0,F_{b2},0,\ldots,F_{bn},0,\ldots,F_{bN},0,F_{bN+1}]^{\mathrm{T}} \tag{9}$$

where F_{bn} is the sub-force vector on the nth bogie ($n = 1$–N):

Fig. 4. View of the Antoing Bridge.

$$\{F_{bn}\} = \begin{cases} P_{Yn} = 2k_{\mathrm{HA}}(Y_{\mathrm{fw}n} + Y_{\mathrm{rw}n}) \\ P_{RXn} = 2k_{\mathrm{HA}}[b_{1n}^2(R_{X\mathrm{fw}n} + R_{X\mathrm{rw}n}) \\ \qquad -h_{3n}(Y_{\mathrm{fw}n} + Y_{\mathrm{rw}n})] \\ P_{RZn} = 2k_{\mathrm{HA}}t_n(Y_{\mathrm{fw}n} - Y_{\mathrm{rw}n}) \\ P_{Zn} = 2k_{\mathrm{VA}}(Z_{\mathrm{fw}n} + Z_{\mathrm{rw}n}) \\ P_{RYn} = 2k_{\mathrm{VA}}t_n(-Z_{\mathrm{fw}n} + Z_{\mathrm{rw}n}) \end{cases}$$

where the subscripts fw$n$ and rw$n$ denote the movements of the front and the rear wheel set of the nth bogie, respectively. The sub-force vector on the $(N+1)$th bogie is:

$$\{F_{b_{N+1}}\} = \begin{cases} P_{Y_{N+1}} = 2k_{\mathrm{HB}}(Y_{\mathrm{fw}N+1} + Y_{\mathrm{rw}N+1}) \\ P_{RX_{N+1}} = 2k_{\mathrm{HB}}[b_{1N+1}^2(R_{X\mathrm{fw}N+1} + R_{X\mathrm{rw}N+1}) \\ \qquad -h_{3N+1}(Y_{\mathrm{fw}N+1} + Y_{\mathrm{rw}N+1})] \\ P_{RZ_{N+1}} = 2k_{\mathrm{HB}}t_{N+1}(Y_{\mathrm{fw}N+1} - Y_{\mathrm{rw}N+1}) \\ P_{Z_{N+1}} = 2k_{\mathrm{VB}}(Z_{\mathrm{fw}N+1} + Z_{\mathrm{rw}N+1}) \\ P_{RY_{N+1}} = 2k_{\mathrm{VB}}t_{N+1}(-Z_{\mathrm{fw}N+1} + Z_{\mathrm{rw}N+1}) \end{cases}$$

The above equations and matrices correspond to the articulated vehicle group. For those of the locomotives with independent bogies (see Ref. [7]).

2.2. Bridge model

The bridge will be modeled by finite elements. The motion equations of the bridge structure can be expressed as:

$$[M_S]\{\ddot{v}_S\} + [C_S]\{\dot{v}_S\} + [K_S]\{v_S\} = \{F_S\} \tag{10}$$

where $[M_S]$, $[C_S]$ and $[K_S]$ are mass, damping and stiffness matrices of the bridge finite element model, $\{v_S\}$ is the nodal displacement vector. $\{F_S\}$ is the force vector on the bridge structure through the vehicle wheel set, in which the force from the ith wheel set can be expressed as:

$$\begin{cases} F_i^Y = 2k_{Hn} \cdot [Y_1 - (-1)^i t_n \cdot R_{Zn} - h_{3n} \cdot R_{Xn} - Y_{i\mathrm{w}n}] \\ F_i^{R_X} = -2k_{Vn} \cdot D \cdot b_{1n}(-R_{Xn} + R_{Xi\mathrm{w}n}) \\ F_i^Z = 2k_{Vn}(Z_n - (-1)^i t_n \cdot R_{Y_n} - Z_{i\mathrm{w}n}) + W_{i\mathrm{w}n} \end{cases} \tag{11}$$

where D is the rail gauge; $W_{i\mathrm{w}n}$ is the static axle load with the subscript $i\mathrm{w}n$ denoting the ith wheel of the nth bogie.

The Antoing Bridge on the Paris–Brussels high speed railway line is taken as an example in the analysis [1] (see Fig. 4). The Antoing Bridge consists of a series of simply supported, PC U shaped girders, which have double tracks. The span length is 50 m, the total length 53.16 m, the total width 18.8 m, the deck width 11.0 m, the side box height 4.3 m, the upper slab thickness 1.1 m, the deck slab thickness 0.7 m and the total mass 3450 t. The eccentric distance of the single track loading to the girder center is 2.25 m. The cross-section of the girder is shown in Fig. 5.

For the U shaped girders, use is made of concrete reinforced cross-wise and prestressed in the direction of the deck spans. The prestressing tendons are positioned across the whole width of the deck slab. Some of them extend through into the web, others are anchored to the ends of the slabs (Fig. 6). The two symmetric side boxes are connected by the deck slab into an integrated cross-section of the girder so that they can work fully together under the action of trains.

The bridge is modeled by three-dimensional volume elements (see Fig. 7). Also a simplified beam model is used. The elasticity of the neoprene bearings is taken into account.

2.3. Wheelset-rail relation

The wheelset-rail relation is established under the following assumptions:

(1) There is no relative displacement between the track and the bridge deck. The elastic effects of the ballast, rail pads and fasteners are neglected. In dealing with bridge vibrations, this assumption is usually adopted by many researchers and has proven to be rational [7,11–14].

The vibration histories of calculated and measured bridge deflections, vertical and lateral accelerations respectively (Figs. 10 and 11, 13 and 14, 16 and 17) show

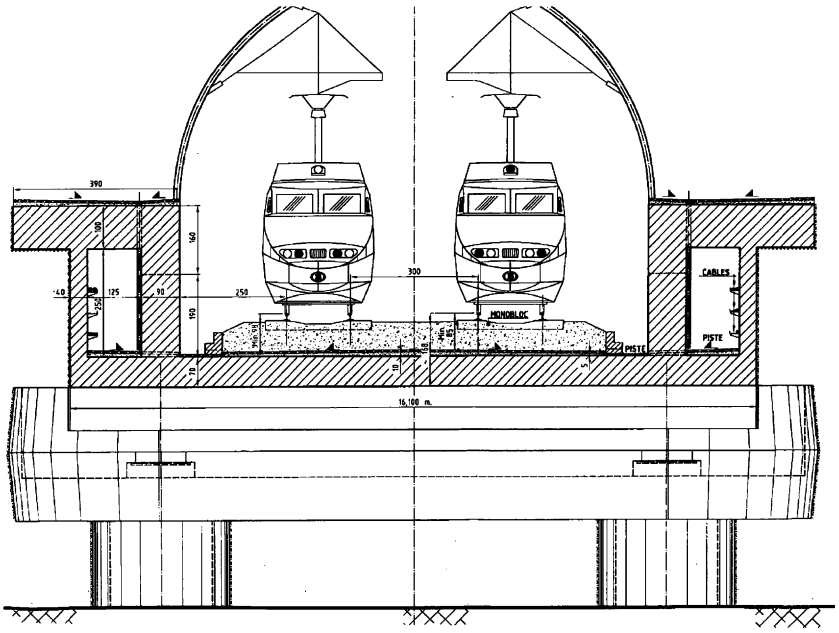

Fig. 5. Cross-section of the U-shaped girder.

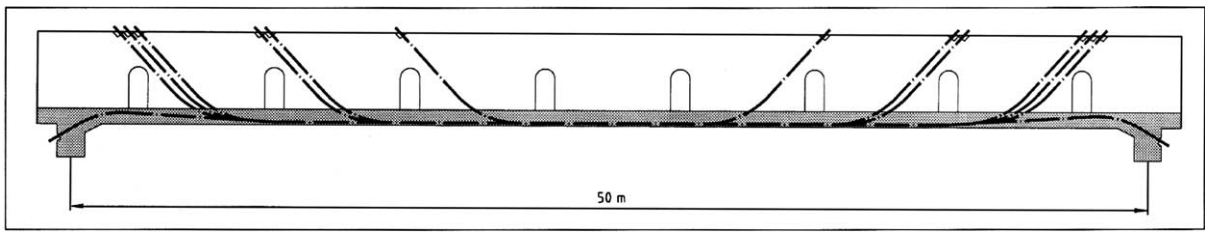

Fig. 6. Prestressing tendon arrangement of the U-shaped girder.

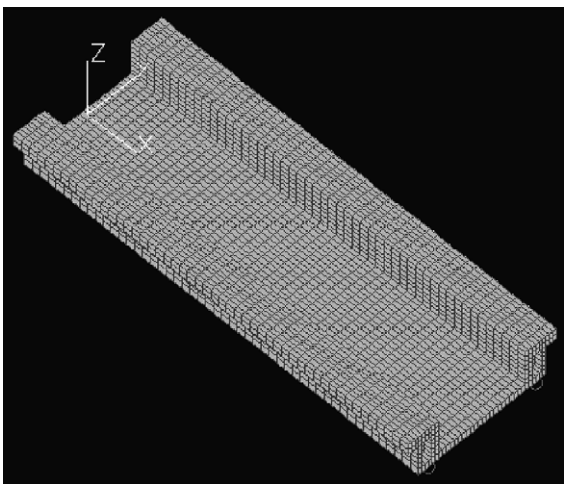

Fig. 7. FE model of the U-shaped girder.

quite good similarities. It can be noticed from Figs. 12, 15 and 18 that the measured data scattered around the corresponding calculated distribution curves versus train speed. In other words, the calculated results are almost at the average position of the distributed measured data at different train speeds. The scattering of the measured data may be owing to the randomness of the system excitation such as the track irregularities. Generally speaking, using the bridge-articulated-train system model under the simplification of track model and other assumptions, the calculated results are well in accordance, both in amplitudes and in distribution tendencies, with the in situ measured data.

(2) The cross-section deformation of the girder is considered in the modal analysis.

According to the assumptions, the displacement, velocity and acceleration of wheelsets are determined by the following relation:

$$\begin{cases} D_w = D_b + D_i + D_h \\ V_w = V_b + V_i + V_h \\ A_w = A_b + A_i + A_h \end{cases} \quad (12)$$

where the subscript w stands for wheelset, b for bridge, i for track irregularity and h for wheelset hunting. D_b, V_b and A_b are displacement, velocity and acceleration at the position of wheelset, including three directions of lateral movement, rolling and floating. The generalized displacement D_b is calculated as following:

$$\begin{cases} Y_b = Y_{b0} + R_{Xb0} \cdot h_4 \\ R_{Xb} = R_{Xb0} \\ Z_b = Z_{b0} \end{cases} \quad (13)$$

where Y, R_X and Z are the displacements in lateral, rotational and vertical directions, respectively; Subscript $b0$ stands for the track center on the girder deck; h_4 is the relative height difference between the deck level and the center of the wheel axles.

In the calculation, the track irregularities are treated as a random series with maximum amplitudes of 4.60 mm in the lateral and 5.77 mm in the vertical direction. The wheel hunting movement has a wavelength of 32 m and an amplitude of 3 mm.

2.4. Calculation method

The Newmark-β algorithm is used in the step-by-step integration of the combined vehicle and bridge system. Being unconditionally convergent, the method does not require a special step length. The generalized displacement, velocity and acceleration of the vehicle and the bridge system within a certain time step are calculated in the program shown in Fig. 8. The convergence of the generalized displacement of each DOF in both systems must be ensured within the step.

3. Calculation results and their comparison to experimental data

The whole response histories of the high speed train passing on one of the double tracks on the bridge were simulated, by using the parameters of the real 50 m trough PC girder and the Thalys train. The train speed range in the calculation is 200–400 km/h and the integration time interval is 0.005 s.

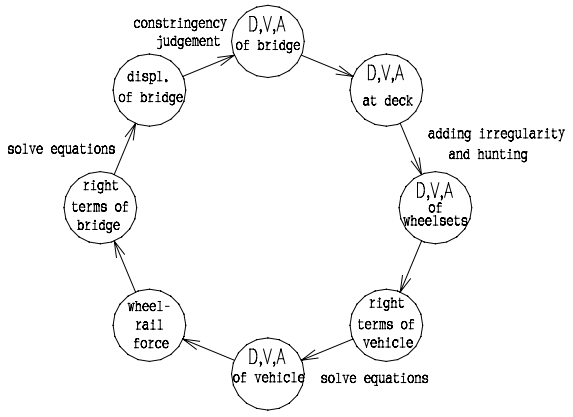

Fig. 8. Flowchart of system iteration program.

The calculated and the measured modal parameters of the girder are given in Table 1 [1].

To understand the dynamic behaviour of the bridge under high speed trains and to verify the analytical model, two in situ experiments on the Antoing Bridge were carried out cooperatively by the Northern Jiaotong University from China and the Catholic University of Leuven, the Free University of Brussels and the Belgium Railway Company NMBS-SNCB in Belgium. Fig. 9 shows the running high speed Thalys train on the bridge during the experiment.

The dynamic response histories of the bridge under the train speed of 300 km/h and the distribution of the maximum bridge responses versus train speed are shown in Figs. 10–18, respectively, where the curves in solid lines are the calculated results and the discrete symbols are the measured data.

Within the train speed range of 200–400 km/h, the maximum deflection of the girder is 1.79 mm, occurring at the resonant train speed of 325 km/h, and the corresponding deflection-to-span ratio is 1/28,000. The

Table 1
Theoretical and experimental modal characteristics

Mode	Eigenfrequency/Hz		Damping ratio/%	Characterization of mode
	Theoretical	Experimental		
B1	3.19	3.19	0.63	First bending (symmetric)
T1	3.95	3.87	2.98	First torsional (symmetric)
S1	6.70	6.84	2.74	First bending of cross-section (symmetric)
B2	9.20	8.77	2.24	First anti-symmetric bending
T2	10.39	10.56	1.83	Second torsional (anti-symmetric)
S2	12.33	12.46	1.52	Second bending of cross-section (anti-symmetric)
B3	14.57	18.56	1.52	Second symmetric bending
B4	18.44	19.28	156	Second anti-symmetric bending

Fig. 9. Dynamic experiment of Antoing Bridge.

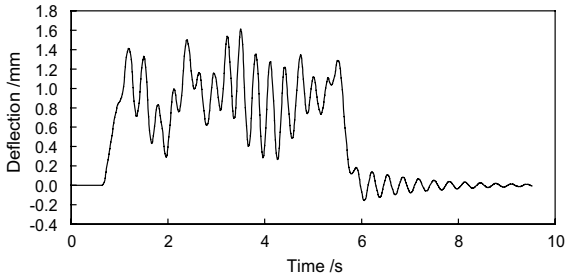

Fig. 10. Calculated deflection history of the girder.

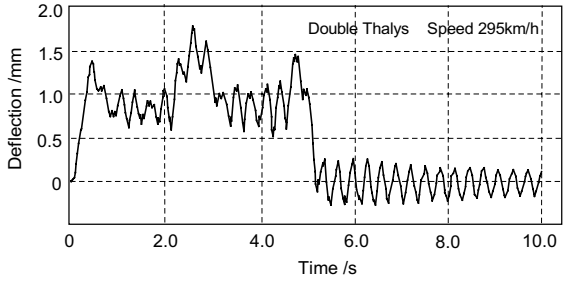

Fig. 11. Measured deflection history of girder.

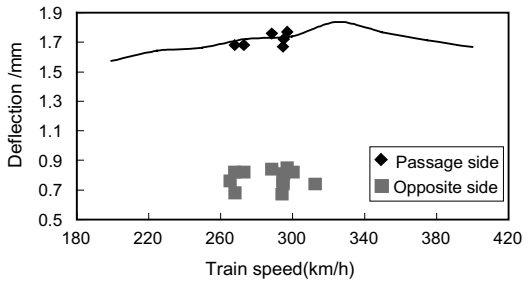

Fig. 12. Distribution of bridge deflection versus train speed.

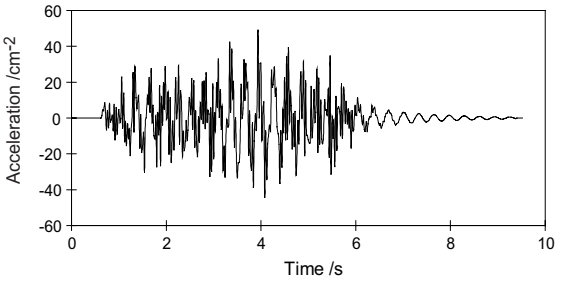

Fig. 13. Calculated vertical acceleration history of girder.

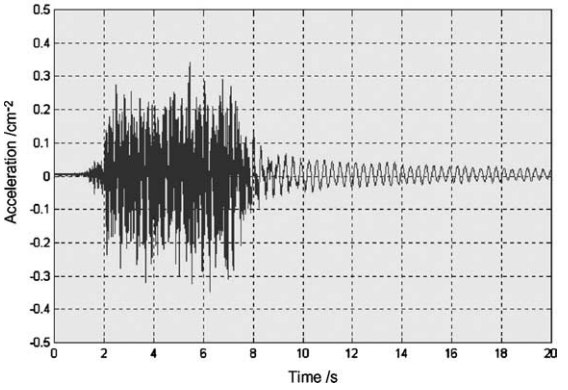

Fig. 14. Measured vertical acceleration history of girder.

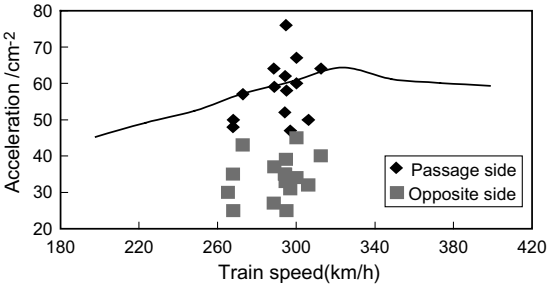

Fig. 15. Vertical bridge acceleration at different train speed.

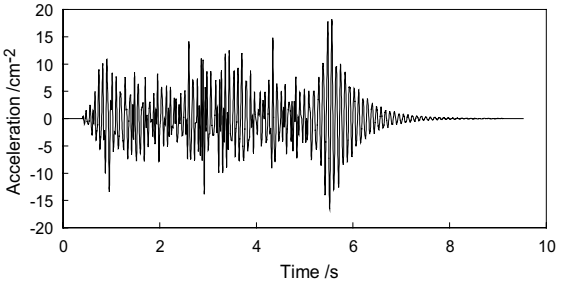

Fig. 16. Calculated lateral acceleration history of girder.

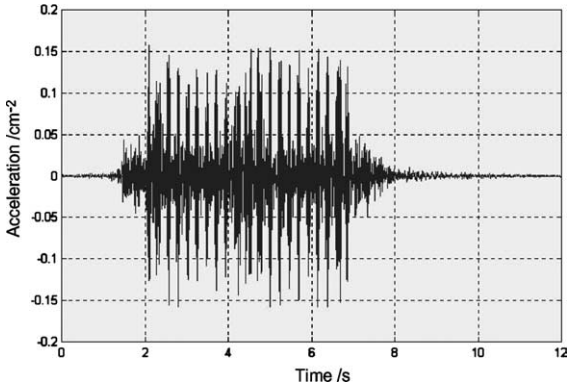

Fig. 17. Measured lateral acceleration history of girder.

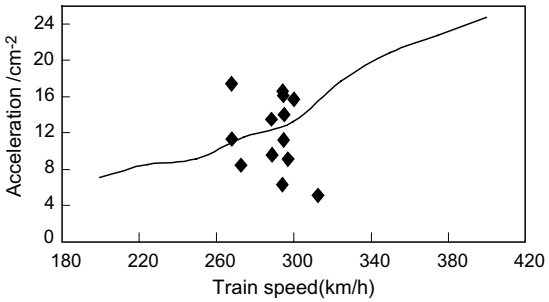

Fig. 18. Lateral bridge acceleration at different train speed.

maximum vertical acceleration of the girder is 0.65 m/s^2.

The lateral amplitudes and the accelerations are very small, and both of them increase with the train speed. In the train speed range lower than 325 km/h, the maximum lateral amplitude is 0.145 mm and the maximum lateral acceleration is 0.167 m/s^2.

Figs. 19 and 20 show the vertical and lateral car-body accelerations of the locomotives and the articulated vehicle under the train speed of 300 km/h. Fig. 21 shows the distribution of the maximum car-body accelerations of the locomotives and the vehicles.

The lateral car-body accelerations of both locomotives and vehicles increase with the train speed. In the train speed range of 200–400 km/h, the maximum lateral car-body accelerations of the locomotives and the vehicles are 1.31 and 0.77 m/s^2, respectively. Both the vertical car-body accelerations of the locomotives and the vehicles are smaller than 0.65 m/s^2. The maximum vertical car-body accelerations of locomotives and vehicles occur at the resonant train speed of 325 km/h.

The study on the 20 vehicles of the double Thalys train reveals that both the lateral and the vertical car-body accelerations of the locomotives are greater than those of the articulated vehicles. The distributions of the

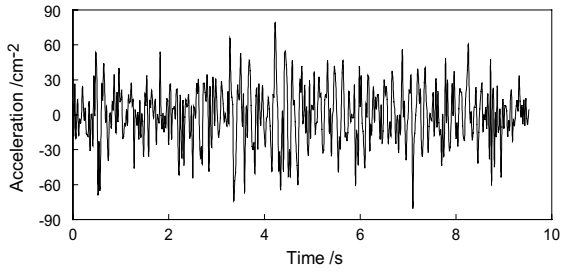

Fig. 19. Vehicle lateral acceleration history.

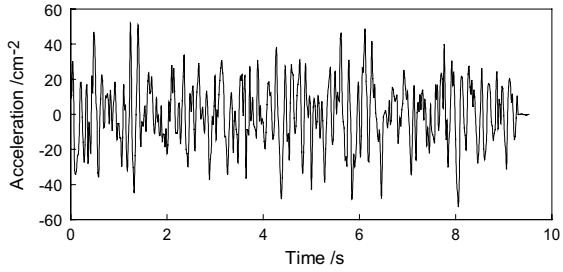

Fig. 20. Vehicle vertical acceleration history.

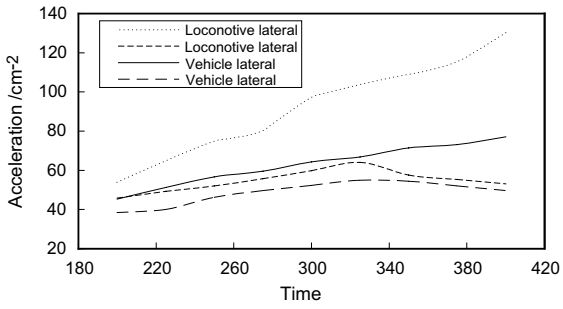

Fig. 21. Distribution of vehicle acceleration versus train speed.

maximum car-body accelerations of the vehicles are shown in Figs. 22 and 23, in which L denotes locomotive, T transition carriage and P articulated vehicles. The car-body accelerations of the vehicles of the 4th and the 5th articulated vehicles are 80–85% in vertical and 70–80% in lateral of those of the transition carriages. These values are similar to those of the 200 km/h railway in China.

The comparisons of the vibration histories of bridge deflections, vertical and lateral accelerations respectively between Figs. 10 and 11, 13 and 14, 16 and 17 show quite good similarities. It can be noticed from Figs. 12, 15 and 18 that the measured data scattered around the corresponding calculated distribution curves versus train speed. In other words, the calculated results are almost at the average position of the distributed measured data

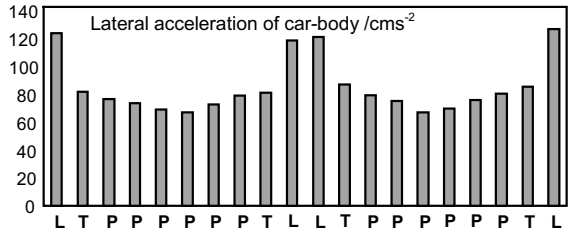

Fig. 22. Maximum lateral accelerations of vehicles.

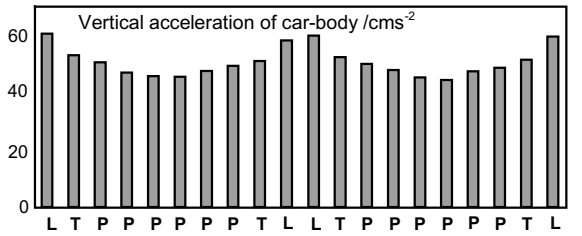

Fig. 23. Maximum vertical accelerations of vehicles.

at different train speeds. The scattering of the measured data may be owing to the randomness of the system excitation such as the track irregularities. Generally speaking, using the bridge-articulated-train system model under the simplification of track model and other assumptions, the calculated results are well in accordance, both in amplitudes and in distribution tendencies, with the in situ measured data.

Compared with the measured results in China, where the trains with non-articulated vehicles are used, the vehicle accelerations are almost the same, while the bridges responses such as deflection–span ratios, amplitudes and accelerations are smaller [16].

In fact, for normal bridges of this length, it is usually more convenient to obtain good results of bridge deflections by using only a load representation of the train [1]. While for the other dynamic responses, such as the accelerations of the bridges, the dynamic responses of the running vehicles, the complete vehicle–bridge system is necessary.

4. Conclusions

The following conclusions can be drawn up from this paper:

(1) The dynamic analytical model of the bridge-articulated-train system and the computer simulation method proposed in this paper can well reflect the main vibration characteristics of the bridge and the articulated train vehicle.

(2) The calculated results are well in accordance, both in response curves, in amplitudes and in distribution tendencies, with the in situ measured data, which verified the effectiveness of the analytical model and the computer simulation method.

(3) The Antoing Bridge has perfect dynamic characteristics. The ratio of deflection-to-span of the Antoing Bridge is smaller than that of the similar bridges in China. The deflections of the girder, the lateral and vertical accelerations of the girder and the car body are in accordance with the currently recognized safety and comfort standards of bridges and running train vehicles.

(4) The articulated train vehicles have a rather good running property at high speed, which also helps to reduce the impact on the bridge structures.

Acknowledgements

This study is sponsored by the National Natural Science Foundation of China (grant no. 50078001) and the Bilateral Research Project (BIL98/09) from the Ministry of the Flemish Community of Belgium.

References

[1] De Roeck G, Maeck J, Teughels A. Train–bridge interaction validation of numerical models by experiments on high-speed railway bridge in Antoing, TIVC'2001, Beijing.
[2] Diana G, Cheli F. Dynamic interaction of railway systems with large bridges. Veh Syst Dynam 1989;18:71–106.
[3] Fryba L. Vibration of solids and structures under moving loads. Groningen: Noordhoff International Publishing; 1972.
[4] Fafard M. Dynamics of bridge vehicle interaction. In: Proc EURODYN'93. Rotterdam: Balkema; 1993. p. 951–60.
[5] Klasztorny M. Vertical vibration of a multi-span bridge under a train moving at high speed. In: Proc EURODYN'99. Rotterdam: Balkema; 1999. p. 651–6.
[6] Li SL, Wang WD. Dynamic analysis of articulated vehicles considering car-body elasticity. J China Railway Sci 1997; 18(2):77–85.
[7] Matsuuta AA. Study of dynamic behaviors of bridge girders for high speed railway. J JSCE 1976;256:35–47.
[8] Shen G, Lu ZG, Hu YS. Nonlinear curving simulation for high speed articulated train. J China Railway Soc 1997; (Suppl):9–14.
[9] Sridharan N, Mallik AK. Numerical analysis of vibration of beams subjected to moving loads. J Sound Vib 1979;65:147–50.
[10] Wiriyachai A, Chu KH, Garg K. Bridge impact due to wheel and track irregularities. J Engng Mech ASCE 1982;108:648–67.
[11] Xia H. Dynamic interaction of vehicles and structures. Beijing: Science Press; 2002.

[12] Xia H, Xu YL, Chan THT. Dynamic interaction of long suspension bridges with running trains. Int J Sound Vibrat 2000;237(2):263–80.
[13] Xia H, De Roeck G, Zhang HR, Zhang N. Dynamic analysis of train–bridge system and its application in steel girder reinforcement. J Comput Struct 2001;79:1851–60.
[14] Yang YB, Yau JD. Vehicle–bridge interaction element for dynamic analysis. J Struct Engng ASCE 1997;123(11): 1512–8.
[15] Zhai WM. Study on coupled vertical dynamics of vehicle–track system. J China Railway Soc 1997;(8):16–21.
[16] Zhang N. Dynamic interaction analysis of vehicle–bridge system under articulated high speed trains. Doctoral Thesis, Beijing, Northern Jiaotong University, 2002.
[17] European Rail Research Institute, List of ERRI publications, January 2003 (available on website http://www.eri.nl).